Modeling Embedded Interpersonal and Multiagent Coordination

Michael J. Richardson[1], Rachel W. Kallen[1], Patrick Nalepka[1], Steven J. Harrison[2], Maurice Lamb[1], Anthony Chemero[1], Elliot Saltzman[3] and R. C. Schmidt[4]

[1]*Center for Cognition, Action and Perception, University of Cincinnati, Cincinnati, OH, U.S.A.*
[2]*School of Health, Physical Education and Recreation, University of Nebraska Omaha, Omaha, NE, U.S.A.*
[3]*Department of Physical Therapy and Athletic Training, Sargent College of Health and Rehabilitation Sciences, Boston University, Boston, MA, U.S.A.*
[4]*Department of Psychology, College of the Holy Cross, Worcester, MA, U.S.A.*

Keywords: Multiagent Systems, Social Coordination, Task Dynamics, Complex Systems, Self-organization.

Abstract: Interpersonal or multiagent coordination is a common part of everyday human activity. Identifying the dynamic processes that shape and constrain the complex, time-evolving patterns of multiagent behavioral coordination often requires the development of dynamical models to test hypotheses and motivate future research questions. Here we review a task dynamic framework for modeling multiagent behavior and illustrate the application of this framework using two examples. With an emphasis on synergistic self-organization, we demonstrate how the behavioral coordination that characterizes many social activities emerges naturally from the physical, informational, and biomechanical constraints and couplings that exist between two or more environmentally embedded and mutually responsive individuals.

1 INTRODUCTION

Many of the everyday movements and actions that individuals perform are accomplished in a social setting and are coordinated with the actions of other individuals. Such behavioral activity is sometimes deliberate and conscious, like when two people are moving a large piece of furniture together, or spontaneous and automatic, such as when two people avoid bumping into one another when walking on a busy sidewalk. It can involve the synchronous coordination of rhythmic movements, such as when individuals synchronize their legs movements while walking and talking, or the asynchronous coordination of complementary or discrete actions, such as when loading a dishwasher together. Finally, multiagent coordination tasks often involve a nested structure of sub-actions, with the varied sequencing of these actions making up the complex syntax of everyday social activity.

The varied complexity of social and multiagent coordination, however, belies the seemingly effortless and robust manner with which human (and many animal) agents are able to perform these activities. Indeed, two or more human agents can often spontaneously coordinate their movements and actions in highly novel task contexts with little to no prior experience or learning. This apparent context insensitivity has led many researchers to focus on trying to identify the invariant set of internal (mental) neurocognitive and perceptual-motor mechanisms that might support effective multiagent coordination across a wide range of task goals and situations (Graf, et al., 2009; Newman-Norland et al., 2007; Vesper et al., 2010). It is becoming increasingly clear, however, that that the CNS cannot "do it all", and that there is more to social action and coordinated multiagent activity than simply neurocognitive processes alone (Coey et al., 2012; Eiler et al., 2013; Knoblich, et al., 2011; Schmidt et al., 2011). This is particularly true for complex multiagent tasks that require individuals to continuously adapt their behavior to each other and to a dynamic task environment, where adopting a purely neurocognitive approach requires increasing appeals to ever higher levels of ungrounded, representational complexity, as well as unsustainable levels of executive control (Chemero, 2009; Schmidt et al., 1990; 2011).

So what other processes or mechanisms might

Richardson, M., Kallen, R., Nalepka, P., Harrison, S., Lamb, M., Chemero, A., Saltzman, E. and Schmidt, R.
Modeling Embedded Interpersonal and Multiagent Coordination.
In *Proceedings of the 1st International Conference on Complex Information Systems (COMPLEXIS 2016)*, pages 155-164
ISBN: 978-989-758-181-6

operate to shape and constrain the complex time-evolving patterns of behavioral coordination that characterize everyday interpersonal or multiagent activity? Here, we propose that many of the stable patterns of interpersonal and multiagent coordination that occur during social activity lawfully emerge from the physical and informational constraints and couplings that exist between two or more environmentally embedded and mutually responsive individuals (Marsh et al., 2009; Richardson and Kallen, 2015; Schmidt et al., 1990; Schmidt et al., 2011). Of particular relevance here is the resultant implication that context dependent multiagent coordination can be understood and modeled as a coupled nonlinear dynamical system. Accordingly, the aim of the current paper is to provide a general overview of how one can employ coupled nonlinear dynamical models to capture and explain the robust, time-evolving structure of Embedded Multi-Agent Dynamics (EMAD). Drawing heavily on the *task* (Saltzman and Kelso, 1987) and *behavioral dynamic* (Warren, 2006) approaches to human behavior, we first briefly define a conceptual framework for modeling EMAD. We then offer paradigmatic examples illustrating how this framework can be employed to formalize low-dimensional, coupled, nonlinear differential equation models of coordinated interpersonal and multiagent behavior.

2 MODELING FRAMEWORK

Consistent with more general nonlinear dynamics and complex systems approaches to human behavior (for reviews see e.g., Kelso, 1995; Richardson et al., 2014; Thelen and Smith, 1994; Warren, 2006), and building on the dynamical interpersonal coordination research of Schmidt and colleagues (e.g., Schmidt et al, 1990; Schmidt and O'Brien, 1997; Schmidt and Turvey, 1994), the framework for modeling EMAD detailed here emphasizes *self-organization* and *contextual emergence*. Accordingly, the stable organization of multiagent behavior is not captured by means of a centralized control structure or neurocognitive mechanism, but rather is modeled as an emergent, *a posteriori* consequence of the distributed interaction of physical processes, informational and neurological couplings, and contextual constraint. Accordingly, stable patterns of behavioral coordination correspond to functional (re)organizations of a multiagent-environment system (e.g., limbs, movements of different actors, objects within a social task environment), one that is temporarily constrained to act as a single coherent unit or *synergy*, formed and destroyed in response to changing task goals and perceived action possibilities (Riley, et al., 2011).

More formally, environmentally embedded interpersonal or multiagent coordination emerges from the activity of two or more agents, $\boldsymbol{A}_i$ (where i = 1, 2, … n agents) in a changing task environment, $\boldsymbol{E}$, via the detection of information, $\boldsymbol{I}$, and the reciprocal and mutually constraining modulation of behavioral action and environmental events by the physical forces, $\boldsymbol{F}$, exerted in the environment by the agents or by other environmental objects or surfaces (or by both).

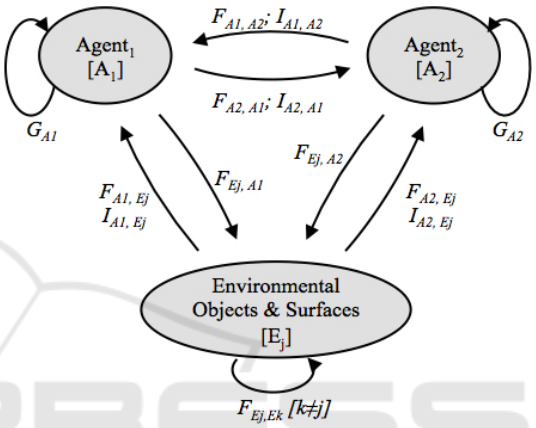

Figure 1: Illustration of a task dynamic framework for modeling Embedded Multi-agent Dynamics (EMAD). See text for details.

A two-agent (interpersonal) illustration of this multiagent-environment modeling framework is illustrated as a system graph in Fig. 1. Here, each agent, i, and task relevant environmental objects and surfaces, j, are represented as nodes, with the different nodes linked via mechanical forces, F, and information, I. Note that an agent's behavior is also a function, G, of intrinsic dynamical or self-referential processes. Similarly, environmental objects or surfaces can also be influenced via physical, F, object-object and object-surface interactions.

This graph representation defines the "bottom-up-all-the-way-down" nature of EMAD, where the general aim of modeling such behavior is to formalize the simplest set of functional relations that give rise to observed macroscopic behavioral order. Different task systems will of course entail different graphs, each needing to be formalized into a specific system of dynamical equations. This is best achieved by defining a functional description of the multiagent task dynamics in terms of an abstract task space. Similar to the intrapersonal task dynamic

formalism of Saltzman and Kelso (1987), this includes appropriately defining (i) the task goal in terms of the relevant terminal objective, (ii) the minimal number of task dimensions (i.e., relevant task axes or variables), which correspond to the active degrees-of-freedom of the task's end-effector, and (iii) the appropriate task dynamics (equations of motion) for each task dimension; equations that should qualitatively capture the movement or action trajectories that are afforded along each task axis of the terminal objective.

Admittedly, defining the relevant task dimensions and appropriate equations of motion for a specific multiagent task is not always easy and can require an extensive amount of empirical research and theorizing, not to mention a considerable amount of trial-and-error. It is with this mind that we have chosen to review a range of simple, yet ubiquitous joint-action tasks and behaviors in order to best illustrate this modeling process and how task dynamic models (specifically with respect to differential equation models) can be formulated to capture and understand the interactive and self-organizing processes that determine coordinated multiagent behavior.

3 RHYTHMIC COLLISION AVOIDANCE

As a first example of how to model the task dynamics of goal directed multiagent coordination, we consider the interpersonal rhythmic collision avoidance task investigated by Richardson et al., (2015). For this task, pairs of naive participants were instructed to continuously move a visual, computer cursor (a small red dot) back and forth between different sets of square target locations, positioned at diagonally opposite corners of a 50" computer monitor. Each participant in a pair stood facing their own computer monitor, which displayed the real-time motion of the participant's own cursor, as well as the motion of their co-participant's cursor. Participants controlled their respective computer cursor using a motion-tracking sensor (see Fig. 2 top). One participant was instructed to continuously move their cursor between the bottom-left and top-right targets while the other participant was instructed to continuously move their cursor between the bottom-right and top-left targets. Most importantly, participants were instructed to produce these continuous cursor motions *without colliding into one another*.

In this task, participant pairs were faced with a conflict between the natural tendency to synchronize straight-line movement trajectories between the targets and the fact that such synchronization would result in a collision. Thus, the research question being investigated was what stable pattern(s) of movement coordination would emerge to ensure task success?

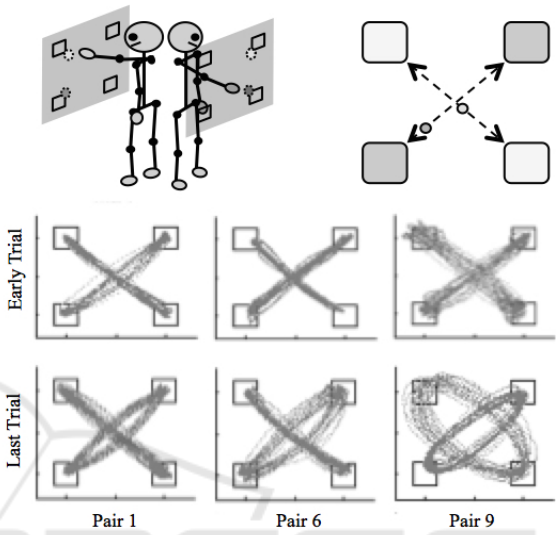

Figure 2: Illustration of the experimental setup (top left) and task display (top right) employed in the Richardson et al (2015) collision avoidance task. (bottom) Prototypical examples of the movement trajectories exhibited by pairs.

Although pairs initially tried to adopt relatively straight line trajectories between the target locations, the results revealed that greater than 90% of pairs quickly converged (by the 3rd or 4th trial) onto a stable task solution that involved complementary task roles, with one participant adopting a more straight-line trajectory between targets and the other participant adopting a more elliptical trajectory between targets (see Fig. 2, bottom). Moreover, the participant who adopted the more elliptical trajectory consistently lagged behind the participant who adopted the more straight-line trajectory by an average of approximately 10° to 30°. Richardson et al., (2015) hypothesized that these complementary behavioral dynamics were the result of a functional asymmetry in the repulsive coupling that prevented collisions, one that not only resulted in an inter-participant asymmetry in the ellipticality of the movement trajectories, but also simultaneously allowed participants to synchronize their between target movements at a phase lag (further increasing the margin of safety). Of particular relevance to our discussion here, is that Richardson et al. were able to

test this hypothesis by developing a task dynamic model of the interpersonal collision avoidance task.

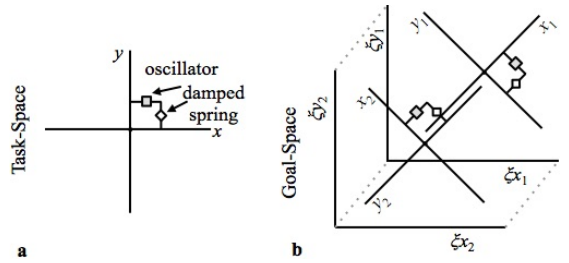

Figure 3: (a) Illustration of the abstract task space axis for the collision avoidance model developed by Richardson, et al., (2015). (b) The task space orientated in the target goal space for a pair of coupled individuals. See text for more details.

Motived by the same task dynamic framework described above, Richardson, et al., (2015) developed this model by defining the terminal objective of each actor's task goal to be a rhythmic motion of the end-effector (i.e., stimulus/end-effector/hand, modeled as a point mass) between two targets within a planar (two-dimensional) task space (see Fig. 3a). In this task space, the *x*-axis corresponded to the axis of instructed direction of oscillation, and was provided with limit cycle (oscillatory) dynamics. The orthogonal task axis, *y*, corresponded to deviations away from the *x*-axis. Given that an actor must minimize these deviations with respect to achieving the instructed task goal, Richardson et al. defined the *y*-axis with simple point-attractor (damped mass-spring) dynamics.

Assuming a point mass of 1 (for simplicity), the functional defined task space was then specified as:

$$\begin{aligned} \ddot{x}_1 - b_{x1}\dot{x}_1 + c_{x1}x_1^2\dot{x}_1 + k_{x1}x_1 &= 0 \\ \ddot{y}_1 + b_{y1}\dot{y}_1 + k_{y1}y_1 &= 0 \end{aligned} \tag{1a}$$

for actor 1 and

$$\begin{aligned} \ddot{x}_2 - b_{x2}\dot{x}_2 + c_{x2}x_2^2\dot{x}_2 + k_{x2}x_2 &= 0 \\ \ddot{y}_2 + b_{y2}\dot{y}_2 + k_{y2}y_2 &= 0 \end{aligned} \tag{1b}$$

for actor 2. Here, x_i and y_i, $y_i, \dot{x}_i$ and $\dot{y}_i, \ddot{x}_i$ and $\ddot{y}_i$ correspond to the position, velocity and acceleration of each actor's end effector (i.e., hand/cursor) along each task axis, respectively. b_{xi} and b_{yi} are the damping coefficients for axis x_i and y_i, respectively, k_{xi} and k_{yi} are stiffness coefficients for axis x_i and y_i, respectively, and $(c_{xi}x_i^2\dot{x}_i)$ is the van der Pol function for axis x_i.

To capture the natural entrainment observed between co-actors, Richardson and colleagues then added an attractive coupling function to each system, similar to what is typically employed for modeling generalized rhythmic (inphase) coordination. That is, they added the diffusive coupling functions

$$\alpha_1(\dot{x}_2 - \dot{x}_1) \tag{2a}$$

and

$$\alpha_2(\dot{x}_1 - \dot{x}_2) \tag{2b}$$

to the equations that define each actor's instructed axes of motion, which resulted in the system

$$\begin{aligned} \ddot{x}_1 - b_{x1}\dot{x}_1 + c_{x1}x_1^2\dot{x}_1 + k_{x1}x_1 \\ = \alpha_1(\dot{x}_2 - \dot{x}_1) \\ \ddot{y}_1 + b_{y1}\dot{y}_1 + k_{y1}y_1 = 0 \\ \ddot{x}_2 - b_{x2}\dot{x}_2 + c_{x2}x_2^2\dot{x}_2 + k_{x2}x_2 \\ = \alpha_2(\dot{x}_1 - \dot{x}_2) \\ \ddot{y}_2 + b_{y2}\dot{y}_2 + k_{y2}y_2 = 0 \end{aligned} \tag{3}$$

It is important to note at this point that Eq. (3) provides an idealized model of inphase interpersonal rhythmic coordination and can be adapted to model the inphase coordination of any two end effectors or point masses (e.g., finger tips; hands, feet, actors) irrespective of the angular orientation of the instructed motion axis. Moreover, other behavioral patterns, such as antiphase coordination and the bistable nature of rhythmic coordination performed in the same direction/plane of motion can also be captured using alternative coupling functions, e.g., as previously identified by Haken et al., (1985) (also see e.g., Dumas et al., 2014; Kelso, 1995; Schmidt and Richardson, 2008)

Based on the behavior of participants at the beginning of the experiment (see Fig. 2), Richardson, et al. (2015) began with the assumption that pairs were initially constrained by the dynamics of Eq. (3). The question then became what minimal changes in the structure of Eq. (3) were required to produce behavior qualitatively similar to that produced by pairs by the end of the experiment? Given that the task instructions were to '*avoid bumping or colliding into each other*', the simplest modification was to add a repelling coupling force that acted on each participant's end-effector to ensure they were repelled from each other. This was accomplished using the repeller functions

$$\gamma_1(x_1 + y_2)e^{-|x_1+y_2|} \tag{4a}$$

$$\gamma_2(x_2 - y_1)e^{-|x_2-y_1|} \tag{4b}$$

for the primary task axes, x_1 and x_2, respectively, and

$$\gamma_1(y_1 - x_2)e^{-|y_1-x_2|} \tag{4c}$$

$$\gamma_2(y_2 + x_1)e^{-|y_2+x_1|} \tag{4d}$$

for the secondary task axes, y_1 and y_2, respectively. In short, these repeller functions push the two participants' end-effectors away from each other, at a strength determined by the parameters, γ_i, and inter-cursor distance, i.e., the exponential terms in Eq. 4 mean that larger (smaller) distances between the participants' cursors result in weaker (stronger) repelling forces (see Richardson et al., 2015 for more details about how these coupling functions were derived). Essentially, if γ_i in participant-*i*'s (*x*, *y*) system is set to zero, the effect of the repeller coupling is null and a straight-line trajectory will be created that is aligned along the participant's limit-cycle axis. However, if γ_i is set to a value greater than zero, the repeller coupling adds a force along both task-axes of participant-*i*, resulting not only in greater ellipticality (due to forces added along the point-attractor task axis), but also in a phase lag relative to participant-*j* when γ_i is greater than γ_j (due to forces added along the limit-cycle task axis).

The complete task dynamic model derived by Richardson et al., (2015) can therefore be written as

$$\begin{aligned} \ddot{x}_1 - b_{x1}\dot{x}_1 + c_{x1}x_1^2\dot{x}_1 + k_{x1}x_1 &= \alpha_1(\dot{x}_2 - \dot{x}_1) - \gamma_1(x_1 + y_2)e^{-|x_1+y_2|} \\ \ddot{y}_1 + b_{y1}\dot{y}_1 + k_{y1}y_1 &= \gamma_1(y_1 - x_2)e^{-|y_1-x_2|} \\ \ddot{x}_2 - b_{x2}\dot{x}_2 + c_{x2}x_2^2\dot{x}_2 + k_{x2} &= \alpha_2(\dot{x}_1 - \dot{x}_2) + \gamma_2(x_2 - y_1)e^{-|x_2-y_1|} \\ \ddot{y}_2 + b_{y2}\dot{y}_2 + k_{y2}y_2 &= -\gamma_2(y_2 + x_1)e^{-|y_2+x_1|} \end{aligned} \quad (5)$$

Importantly, this system was not only able to successfully capture the stable asymmetric task solution adopted by participants—namely, asymmetric movement trajectories and phase-lagged rhythmic synchronization—but it could also capture the different types of successful and unsuccessful movement solutions adopted by participants pairs throughout the course of the experiment.

Essentially, there are three qualitative types of movement trajectories that can be generated from Eq. (5). These are displayed in Fig. 4 and depend on the magnitudes of γ_1 and γ_2 and the degree that $\gamma_1 \neq \gamma_2$. First, if $\gamma_1 = \gamma_2 = 0$, then no motion is created along y_1 or y_2 (i.e. $\dot{y}_1 = \dot{y}_2 = 0$), which makes the behavior of Eq. (5) equivalent to the behavior of Eq. (3). This corresponds to straight-line inphase coordination (Fig. 4 left) and as noted previously was what most participants in the Richardson et al study spontaneously produced at the beginning of the experiment—albeit to the detriment of success, in that such behavior leads to collisions.

The second qualitative type of movement trajectories exhibited by Eq. (5) occur when $\gamma_1 \neq \gamma_2$. As can be seen from an inspection of the right panel of Fig. 4, when $\gamma_1 \neq \gamma_2$ an asymmetry in the between target movement trajectories emerges, as well as a phase lag between the more elliptical and the more straight-line trajectory. This behavioral pattern is similar to the successful task solution adopted by pairs in the Richardson et al. study and is consistent with the hypothesis that participants adopted an asymmetric relation in coupling in order to avoid collisions and simultaneously synchronize their between target movements.

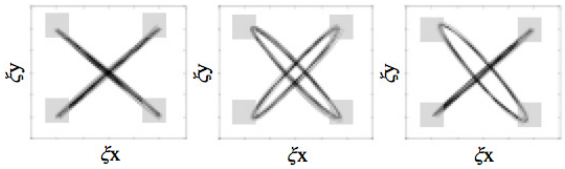

Figure 4: Examples of the three qualitative types of movement trajectories that can be produced by the Richardson et al., (2015) collision avoidance model, Eq. (5), for various settings of the parameters of γ_1 and γ_2(see text for more details).

Lastly, if $\gamma_1 = \gamma_2 > 0$, then equivalent motion patterns are created along y_1 and y_2 resulting in elliptical trajectories that are symmetric across participants and synchronized with zero phase lag between the participants' limit cycle axes. Interestingly, this third situation also results in a stable collision avoidance solution, especially for $\gamma_1 = \gamma_2 >> 0$, but one that does not include a phase lag between the limit-cycle axes and, hence, has a lower 'margin of safety' than the asymmetric solution adopted by participants for the second qualitative type of movement pattern described above.

The third type of task solution was observed in a follow-up study (Eiler et al., 2015), in which the participants were not penalized for collisions. Under these conditions, participant pairs also produced movements with less ellipticality. That is, pairs produced a more symmetrical pattern of elliptical inphase coordination with a smaller degree of ellipticality than when collisions were penalized. Given Eq. (5), this suggests that decreasing the cost of failure not only weakened the repulsive coupling between participants, but also resulted in pairs employing similar magnitudes of repulsive avoidance (i.e., $\gamma_1 \approx \gamma_2 > 0$).

Most recently, Eiler et al., (2015) have also demonstrated how Eq. (5) can predict the types of patterns exhibited between pairs of individuals walking or running back and forth between target

locations in a real 3-dimensional space. Specifically, Eiler et al., instructed pairs of participants to walk or run at a comfortable pace back and forth between sets of target landmarks positioned in a cross-type arrangement (see Fig. 5, left). The distance between the participants' target landmarks were also manipulated, with the landmarks positioned either 3 meters or 5 meters apart. Of particular significance, was that the 2 (speed: walk vs. run) by 2 (distance: 3 vs. 5 m) within subjects design employed in this study essentially mapped onto different "chances/severity" of collision conditions, with walking between targets positioned 5 m apart having the lowest chance/severity of collision and running between targets positioned 3 m apart having the highest chance/severity of collision.

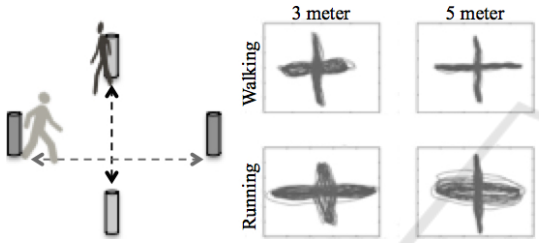

Figure 5: (left) experimental setup for the walking and running collision avoidance task investigated by Eiler et al., (2015). (right) Example movement trajectories for the different target distance and pace conditions explored.

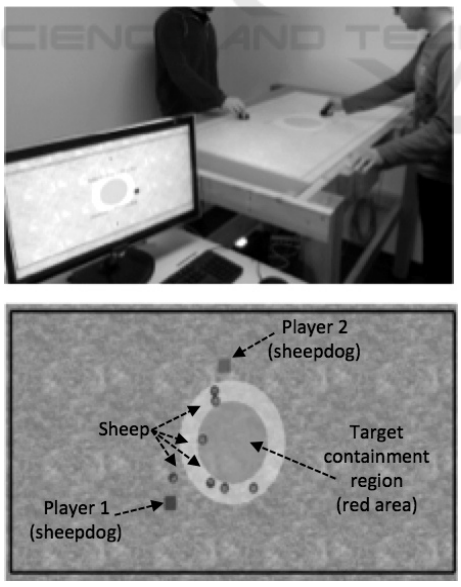

Figure 6: Experimental setup (top) and birds-eye view of game field (bottom) for the sheepdog game investigated by Nalepka et al., (2015).

As expected, the degree to which pairs adopted synchronous straight line or elliptical movement trajectories between the target locations, as well as the symmetry of the co-actors movement trajectories, was a function of these chance/severity of collision manipulations (see Figure 5, right)—patterns that could be captured by Eq. (5) by modulating limit-cycle axis frequency (i.e., k_{xi} and k_{yi}) and the magnitude and symmetry of the repulsive coupling parameters γ_i.

4 MULTIAGENT HERDING

As a second example of how task dynamic modeling can be employed to understand EMAD, we consider the multiagent sheepdog herding game recently investigated by Nalepka et al., (2015). This game required pairs of naïve participants to work together to contain groups of 3, 5, or 7 virtual sheep (i.e. small, 'wool'-covered balls) within a central target region of a virtual field presented on a large tabletop display (see Fig. 6). The sheep's' movements were governed by random Brownian motion dynamics and were repelled away from virtual dogs (a blue or red colored box) that the participants' controlled in real-time using hand-held motion tracking sensors. Specifically, the participants held the sensors in their hands on top of the colored boxes (dogs) projected on the tabletop display, essentially making their hand the "sheepdog".

Initially all participants pairs adopted a kind of search and recover strategy, in which each individual would move toward and corral the furthest sheep from the center of the game field on their side

However, when a pair's search and recover performance improved to the point where they could consistently and effectively corral the sheep into the target region in the center of the game field, most pairs spontaneously transitioned to a coupled oscillator containment strategy, in which the participants synchronously moved back and forth in a semicircular inphase or antiphase manner around the target containment region—establishing a kind of "spatiotemporal" wall around the sheep. The two modes of behavior are illustrated in Figure 7.

Given that nearly all participant pairs spontaneously adopted the search and recover strategy at the very beginning of the experiment(participants could not talk during the experiment) and then, over the course of repeated performance, also discovered the coupled oscillatory containment strategy, Nalepka, et al., concluded that both behavioral modes were entailed by the constraints, goals and inter-agent couplings that defined the multiagent sheep herding game.

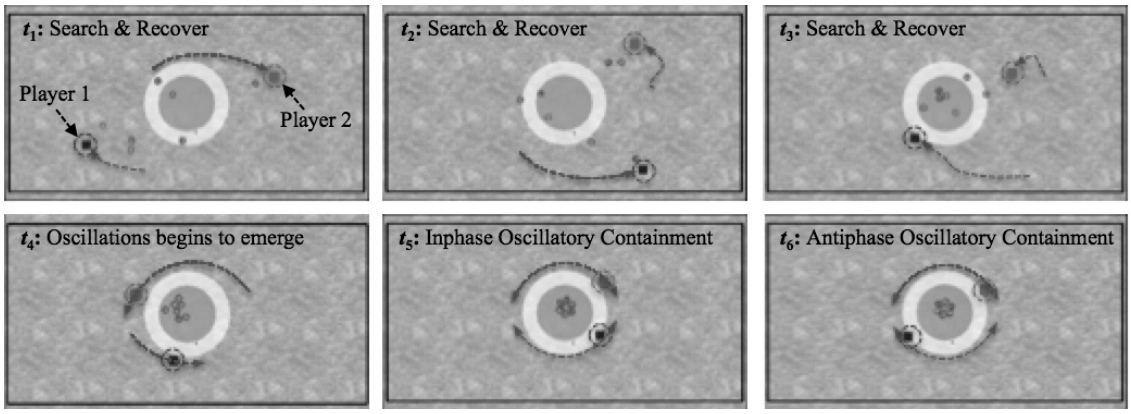

Figure 7: Time lapsed (t1…t6) illustrations of the two behavioral modes exhibited by pairs in the sheepdog herding game. Dashed arrows indicate movement direction. Dashed circles highlight participant (sheepdog) position of the table, moving from sheep to sheep in an attempt to get all of the sheep within the central target area and then keep them there.

In other words, the behavioral modes adopted (and discovered) by participants were both stabilities of the games task dynamics. Furthermore, finding that the stable patterns of synchronized oscillatory containment were consistent with the stabilities of intra- and interpersonal rhythmic coordination (e.g., Haken et al., 1985; Kelso, 1995; Schmidt et al., 1990; Schmidt et al., 1998; Richardson et al., 2007)——namely, stable inphase and antiphase behavior was observed, with inphase coordination occurring more frequently and more stably than antiphase coordination—also led Nalepka and colleagues to conclude that the underlying dynamical system should entail a corresponding coupled oscillator process.

In support of these conclusions, Nalepka, et al. have been developing a simple task dynamic model of the sheepdog game that not only captures (i) both behavioral modes within the same system of equations of motion and (ii) the prototypical dynamics of interpersonal rhythmic coordination (i.e., coupled oscillators), but also (iii) the possibility for a spontaneous transition between the two behavioral modes as a function of a sheep-distance dependent Hopf bifurcation (here we present a preliminary version of the model that has been developed to date). As illustrated in Fig. 8, the preliminary model (still to be completely validated) captures the terminal objective of a participants' behavior with respect to the center of containment region within the ξ_x and ξ_y game space. Here, x_i is the oscillatory perimeter path of each participant *i's* hand, where i = 1 or 2, with respect to half (π-radians) of the target containment region of success closest to the participant's side of the game space. y_i corresponds to the radial distance of each participant from the center of the game space and θ_i is the radial angle of each participant from the center of the game space defined with respect to the ξ_y polar axis on each participants side of the table (i.e., $+\xi_y$ for participant 1 and $-\xi_y$ for participant 2). Thus, each participant's perimeter path, x_i, is centered on the participants radial (y_i, θ_i) position within the (ξ_x, ξ_y) game space.

To be consistent with the previous research modeling the dynamics of rhythmic arm and hand movements (Kay et al., 1987), and rhythmic interlimb and interpersonal coordination (Haken, et al., 1985; Schmidt and Richardson, 2008), the topology of the x_i perimeter path movement was defined using a set of coupled hybrid nonlinear oscillators of the form

$$\begin{aligned} &\ddot{x}_1 + \alpha_1\dot{x}_1 + \beta_1 x_1^3 + \gamma_1 x_1^2\dot{x}_1 + \omega_1^2 x_1 \\ &\quad = (\dot{x}_1 - \dot{x}_2)(A - B(x_1 - x_2)^2) \\ &\ddot{x}_2 + \alpha_2\dot{x}_2 + \beta_2 x_2^3 + \gamma_2 x_2^2\dot{x}_2 + \omega_2^2 x_2 \\ &\quad = (\dot{x}_2 - \dot{x}_1)(A - B(x_2 - x_1)^2) \end{aligned} \tag{6}$$

with the positive/negative (excitatory/inhibitory) damping parameters α_1 and α_2, scaled as a function of sheep distance using the equation

$$\dot{\alpha}_i = \delta_i(\varphi_{sd,i(t)}^2 - C_{sd,i} - \alpha_i) \tag{7}$$

For Eq. 6, x_i and x_i, $\dot{x}_i$ and $\dot{x}_i$, $\ddot{x}_i$ and $\ddot{x}_i$ correspond to the position, velocity and acceleration of each agent's hand along the x_i path, ω_i^2 defines the stiffness or frequency of movement along the corresponding x_i path, and the functions ($\beta_i x_i^3$) and ($\gamma_i x_i^2 \dot{x}_i$) corresponding to Rayleigh and van der Pol escapements terms, respectively. The coupling function to the right of the equals sign in each equation is the same as that previously derived by Haken et al., (1985), and defines both inphase (0°) and antiphase (180°) relative phase relationships as the stable coordination modes between the two

oscillators (when α_1 and α_2 < 0), whose relative strength is defined by the parameters *A* and *B*.

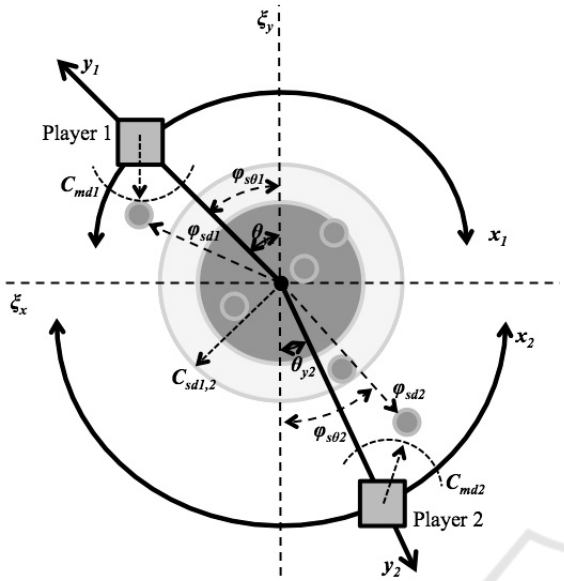

Figure 8: Illustration of the task space employed for the sheep-herding model which captures player i's (where i = 1 or 2) sheepdog location at any time within the ξ_x and ξ_y planar game space in polar coordinates (y_i, θ_i), with y_i corresponding to the radial distance of player i from the center of the ξ_x and ξ_y planar game space and θ_i corresponding to player i's radial angle (± 90°) from the ξ_y game space axis on their side of the game field. x_i is the oscillatory perimeter path of each participant i's sheepdog with respect to half (π-radians) of the target containment region of success closest to the participant's side of the game space, such that each participant's perimeter path, x_i, is centered on the participants radial (y_i, θ_i) position within the (ξ_x, ξ_y) game space (see text for more details).

Central to the switch between the search and recover and oscillatory containment modes of behavior is the Hopf bifurcation that occurs for each oscillator system, x_i, when α_i is decreased from a positive to a negative value. That is, when $\alpha_i > 0$, x_i behavior is that of a nonlinear damped mass spring with a stable fixed-point solution. However, when $\alpha_i < 0$, x_i behavior is that of a nonlinear limit cycle oscillator.

As defined in Eq. (7), the value of α_i at any instance in time, (*t*), is a differential function of the distance, $\varphi_{sd,i(t)}$, of the furthest sheep on participant *i*'s side of the game space with respect to a maximum safe containment distance, $C_{sd,i}$ and a fixed rate of change parameter δ_i. Accordingly, when the distance, $\varphi_{sd,i(t)}$, of the sheep furthest from the center of the game space on participant *i*'s side of the game space is outside participant *i*'s maximum safe containment distance, $C_{sd,i}$, $\alpha_i > 0$ and behavior along the x_i corresponds to that of a nonlinear mass damped spring. Conversely, when the distance, $\varphi_{sd,i(t)}$, of the sheep furthest from the center of the game space on participant *i*'s side of the game space is inside participant *i*'s maximum safe containment distance, $C_{sd,i}$, $\alpha_i < 0$ and behavior along the x_i corresponds to that of a nonlinear limit cycle oscillator.

A participant's radial distance, y_i, was defined as

$$\ddot{y}_i + b_{yi}\dot{y}_i + \varepsilon_i\left(y_i - (\varphi_{sd,i(t)} + C_{md,i})\right) = 0 \qquad (8)$$

with the radial orientation θ_i defined by

$$\ddot{\theta}_i + b_{\theta i}\dot{\theta}_i + \mu_i\left(\theta_i - \varphi_{s\theta,i(t)}D_{sd,i}\right) = 0 \qquad (9)$$

Here, $\dot{y}_i$ and $\ddot{y}_i$, and $\dot{\theta}_i$ and $\ddot{\theta}_i$ correspond to the velocity and acceleration of participant *i*'s radial distance and radial orientation from the center of the game space, respectively. $\varphi_{sd,i(t)}$ is again the distance of the furthest sheep on participant *i*'s side of the game space and $\varphi_{s\theta,i(t)}$ is the angle of the furthest sheep on participant *i*'s side of the game space relative to corresponding ξ_y polar game space axis. $C_{md,i}$ is a fixed parameter the sets minimum preferred distance that a participant likes to approach a sheep, and ε_i and μ_i scale the force (rate) at which participant *i* minimizes the difference between the radial distance and radial angle of their sheepdog and the radial distance and angle of the furthest sheep from the center of the game space on their side of the game field, respectively. Finally, $D_{sd,i}$ is a Heaviside parameter defined as

$$D_{sd1} = \begin{cases} 0, & \varphi_{sd,1(t)} \leq C_{sd,1} \\ 1, & \varphi_{sd,1(t)} > C_{sd,1} \end{cases} \qquad (10)$$

which results in the stable fixed point solution $\theta_{i,stable} = 0$, when all of the sheep on participant *i*'s side of the game space are within the participant's maximum safe containment distance, $C_{sd,i}$. Thus, when all of the sheep on participant *i*'s side of the game space are within the region of containment, the radial orientation θ_i approaches zero for participant *i* and their corresponding x_i path is centered about ξ_y.

Collectively, the task dynamic model of the (bi-agent) sheepherding game can be written as follows,

$$
\begin{aligned}
&\ddot{y}_1 + b_{y1}\dot{y}_1 + \varepsilon_1\left(y_1 - (\varphi_{sd,1(t)} + C_{md,1})\right) = 0 \\
&\ddot{\theta}_1 + b_{\theta 1}\dot{\theta}_1 + \mu_1\left(\theta_1 - \varphi_{s\theta,1(t)} D_{sd,1}\right) = 0 \\
&\ddot{x}_1 + \alpha_1 \dot{x}_1 + \beta_1 x_1^3 + \gamma_1 x_1^2 \dot{x}_1 + \omega_1^2 x_1 \\
&\quad = (\dot{x}_1 - \dot{x}_2)(A \\
&\quad - B(x_1 - x_2)^2) \\
&\dot{\alpha}_1 = \delta_1(\varphi_{sd,1(t)}^2 - C_{sd,1} - \alpha_1) \\
&D_{sd1} = \begin{cases} 0, & \varphi_{sd,1(t)} \le C_{sd,1} \\ 1, & \varphi_{sd,1(t)} > C_{sd,1} \end{cases} \\
&\ddot{y}_2 + b_{y2}\dot{y}_2 + \varepsilon_2\left(y_2 - (\varphi_{sd,2(t)} + C_{md,2})\right) = 0 \\
&\ddot{\theta}_2 + b_{\theta 2}\dot{\theta}_2 + \mu_2\left(\theta_2 - \varphi_{s\theta,2(t)} D_{sd,2}\right) = 0 \\
&\ddot{x}_2 + \alpha_2 \dot{x}_2 + \beta_2 x_2^3 + \gamma_2 x_2^2 \dot{x}_2 + \omega_2^2 x_2 \\
&\quad = (\dot{x}_2 - \dot{x}_1)(A \\
&\quad - B(x_2 - x_1)^2) \\
&\dot{\alpha}_2 = \delta_2(\varphi_{sd,2(t)}^2 - C_{sd,2} - \alpha_2) \\
&D_{sd2} = \begin{cases} 0, & \varphi_{sd,2(t)} \le C_{sd,2} \\ 1, & \varphi_{sd,2(t)} > C_{sd,2} \end{cases}
\end{aligned}
\tag{11}
$$

Importantly, not only does this model effectively capture the bimodal behavior exhibited by pairs in the experimental study, but it is also resistant to perturbations in the sheep movement and location and is able to spontaneously transition between the search and recover and oscillatory containment behavioral modes via a sheep distance dependent Hopf bifurcation process. Videos presenting example demonstrations and simulations of the model, as well as a real participant behavior can be viewed at: http://www.emadynamics.org/bi-agent-sheep-herding-game/.

5 CONCLUSION

Our aim here was to provide a brief overview of how EMAD can be modeled and understood using a task dynamic framework. It is important to appreciate that the goal of dynamical modeling is not to perfectly simulate the exact trajectory or end state of system behavior, but to shed light on the structural relations and self-organizing processes that give rise to effective and robust behavior. Indeed, the power of a task dynamical model rests on its ability to validate hypotheses, generate testable predictions, and motivate future research questions. It is in this way that developing self-organized task dynamic models have the potential to uncover the fundamental processes that shape and constrain human behavior in general.

ACKNOWLEDGEMENTS

The research was supported by National Institutes of Health, R01GM105045.

REFERENCES

Chemero, A., 2009. Radical embodied cognitive science. Boston, MA: MIT Press.

Coey, C., Varlet, M., Richardson, M. J., 2012. Coordination dynamics in a socially situated nervous system. *Frontiers in human neuroscience. 6*, 164.

Dumas, G., de Guzman, G. C., Tognoli, E., Kelso, J. S., 2014. The human dynamic clamp as a paradigm for social interaction. *Proceedings of the National Academy of Sciences*, *111*(35), E3726-E3734.

Eiler, B., Coey, C. A., Ariyabuddhiphongs, K., Kallen, R. W., Harrison, S. J., Saltzman, E., Schmidt, R. C., Richardson, M. J., 2015. Poster presented at the 5th Joint Action Meeting, Budapest, Hungary, July 2015.

Eiler, B., Kallen, R. W., Harrison, S. J., Saltzman, E., Schmidt, R. C., Richardson, M. J., 2015. Behavioral Dynamics of a Collision Avoidance Task: How Asymmetry Stabilizes Performance. In Noelle, D. C., Dale, R., Warlaumont, A. S., Yoshimi, J., Matlock, T., Jennings, C. D., & Maglio, P. P. (Eds.) *Proceedings of the 37th Annual Meeting of the Cognitive Science Society*. Austin, TX: Cognitive Science Society.

Eiler, B., Kallen, R. W., Harrison, S. J., Richardson, M. J., 2013. Origins of Order in Joint Activity and Social Behavior. *Ecological Psychology, 25*, 316–326.

Graf, M., Schütz-Bosbach, S., Prinz, W., 2009. Motor Involvement in Action and Object Perception Similarity and Complementarity. In G. Semin, & G. EchterhoV (Eds), *Grounding sociality: Neurons, minds, and culture*. NY: Psychology Press.

Haken, H., Kelso, J. A. S., Bunz, H., 1985. A theoretical model of phase transitions in human hand movements. *Biological Cybernetics, 51*, 347-356.

Kay, B. A., Kelso, J. A., Saltzman, E. L., Schöner, G. (1987). Space–time behavior of single and bimanual rhythmical movements: Data and limit cycle model. *Journal of Experimental Psychology: Human Perception and Performance*, *13*(2), 178.

Kelso, J. A. S., 1995. *Dynamic patterns.* Cambridge, MA: MIT Press.

Knoblich, G., Butterfill, S., Sebanz, N., 2011. Psychological research on joint action: theory and data. In B. Ross (Ed.), *The Psychology of Learning and Motivation, 54* (pp. 59-101), Burlington: Academic Press.

Marsh, K. L., Richardson, M. J., Schmidt, R. C., 2009. Social connection through joint action and interpersonal coordination. *Topics in Cognitive Science, 1*, 320-339.

Nalepka, P., Riehm, C., Mansour, C. B., Chemero, A., Richardson, M. J., 2015. Investigating Strategy Discovery and Coordination in a Novel Virtual Sheep

Herding Game among Dyads. In Noelle, D. C., Dale, R., Warlaumont, A. S., Yoshimi, J., Matlock, T., Jennings, C. D., Maglio, P. P. (Eds.) *Proceedings of the 37th Annual Meeting of the Cognitive Science Society*. Austin, TX: Cognitive Science Society.

Newman-Norlund RD, Noordzij, ML, Meulenbroek, R.G.J, Bekkering H., 2007. Exploring the brain basis of joint action: Co-ordination of actions, goals and intentions. *Social Neuroscience, 2*, 48-65.

Richardson, M. J. Dale R., Marsh, K. L., 2014. Complex Dynamical Systems in Social and Personality Psychology: Theory, Modeling and Analysis. In H. T. Reis, and C. M. Judd. (Eds.). *Handbook of Research Methods in Social and Personality Psychology, 2nd Edition.* New York, NY: Cambridge University Press.

Richardson, M. J., Kallen, R. W., 2015. Symmetry-Breaking and the Contextual Emergence of Human Multiagent Coordination and Social Activity. In E. Dzhafarov, S. Jordan, R. Zhang, and V. Cervantes (Eds.). *Contextuality from Quantum Physics to Psychology*. (pp. 229-286). World Scientific.

Richardson, M. J., Harrison, S. J., Kallen, R. W., Walton, A., Eiler, B., Schmidt, R. C., 2015. Self-Organized Complementary Coordination: Dynamics of an Interpersonal Collision-Avoidance Task. *Journal of Experimental Psychology: Human Perception and Performance.*

Richardson, M. J., Marsh, K. L., Isenhower, R., Goodman, J., Schmidt, R. C., 2007. Rocking together: Dynamics of intentional and unintentional interpersonal coordination. *Human Movement Science, 26*, 867-891.

Riley, M. A., Richardson, M. J., Shockley, K. Ramenzoni, V. C., 2011. Interpersonal Synergies. *Frontiers in Psychology, 2,* 1-7.

Saltzman, E. L., Kelso, J. A. S. (1987). Skilled actions: A task dynamic approach. *Psychological Review, 94*, 84–106.

Schmidt, R. C., Bienvenu, M., Fitzpatrick, P. A., Amazeen, P. G., 1998. A comparison of within- and between-person coordination: Coordination breakdowns and coupling strength. *Journal of Experimental Psychology: Human Perception and Performance*, *24*, 884-900.

Schmidt, R. C., Carello, C., Turvey, M. T., 1990. Phase transitions and critical fluctuations in the visual coordination of rhythmic movements between people. *Journal of Experimental Psychology: Human Perception and Performance*, *16*, 227-247.

Schmidt, R. C., Fitzpatrick, P., Caron, R., Mergeche, J., 2011. Understanding social motor coordination. *Human Movement Science*, *30*, 834-845.

Schmidt, R. C., O'Brien, B., 1997. Evaluating the dynamics of unintended interpersonal coordination. *Ecological Psychology*, *9*, 189-206.

Schmidt, R. C., Richardson, M. J., 2008. Dynamics of Interpersonal Coordination. In A. Fuchs & V. Jirsa (Eds.). *Coordination: Neural, Behavioral and Social Dynamics*. (pp. 281-308). Heidelberg: Springer-Verlag.

Schmidt, R. C., Turvey, M. T., 1994. Phase-entrainment dynamics of visually coupled rhythmic movements. *Biological Cybernetics*, *70*, 369-376.

Vesper, C., Butterfill, S., Knoblich, G., Sebanz, N., 2010. A minimal architecture for joint action. *Neural Networks, 23,* 998-1003.

Warren, W. H. (2006). The Dynamics of Perception and Action. *Psychological Review, 113*, 358–389.